

## EFFICIENCY AND RADIATIVE RECOMBINATION RATE ENHANCEMENT IN GAN/ALGAN MULTI-QUANTUM WELL-BASED ELECTRON BLOCKING LAYER FREE UV-LED FOR IMPROVED LUMINESCENCE

Samadrita Das<sup>1</sup>, Trupti R. Lenka<sup>1</sup>, Fazal A. Talukdar<sup>1</sup>,  
Ravi T. Velpula<sup>2</sup>, Hieu P. T. Nguyen<sup>2</sup>

<sup>1</sup>Department of Electronics and Communication Engineering,  
National Institute of Technology Silchar, Assam, 788010, India

<sup>2</sup>Department of Electrical and Computer Engineering,  
New Jersey Institute of Technology Newark, New Jersey, 07102, USA

**Abstract.** *In this paper, an electron blocking layer (EBL) free GaN/AlGaIn light emitting diode (LED) is designed using Atlas TCAD with graded composition in the quantum barriers of the active region. The device has a GaN buffer layer incorporated in a c-plane for better carrier transportation and low efficiency droop. The proposed LED has quantum barriers with aluminium composition graded from 20% to ~2% per triangular, whereas the conventional has square barriers. The resulted structures exhibit significantly reduced electron leakage and improved hole injection into the active region, thus generating higher radiative recombination. The simulation outcomes exhibit the highest internal quantum efficiency (IQE) (48.4%) indicating a significant rise compared to the conventional LED. The designed EBL free LED with graded quantum barrier structure acquires substantially minimized efficiency droop of ~7.72% at 60 mA. Our study shows that the proposed structure has improved radiative recombination by ~136.7%, reduced electron leakage, and enhanced optical power by ~8.084% at 60 mA injected current as compared to conventional GaN/AlGaIn EBL LED structure.*

**Key words:** *Ultra-violet (UV), light emitting diode (LED), gallium nitride (GaN), internal quantum efficiency (IQE), multi-quantum well (MQW), quantum barrier (QB), electron blocking layer (EBL)*

### 1. INTRODUCTION

Ultra-violet light emitting diodes (LEDs) are of immense importance because of their potential applications and have attracted considerable attention in optical communication, pharmaceutical appliances, water and air purification, and many more. Gallium Nitride (GaN),

---

Received June 28, 2022; revised July 14, 2022, and July 26, 2022; accepted July 26, 2022

**Corresponding author:** Samadrita Das

Department of Electronics and Communication Engineering, National Institute of Technology Silchar, Assam, India

E-mail: samadrita\_rs@ece.nits.ac.in

a promising material for generating UV luminescence over a wide range of spectrum, has attracted many researchers' attention [1]–[4]. GaN shows a wide band gap ranging from 0.7 eV, 3.4 eV to 6.2 eV which can further be amplified by introducing aluminum (Al) to prepare AlGa<sub>N</sub> alloy [5], [6]. Moreover, GaN being an environmental friendly material has better biocompatibility and low manufacturing price [7]–[11]. GaN are used for creating high-efficiency shorter wavelength luminescence and fabricate semiconductor based materials such as LED, laser diode (LD) with low threshold [12], [13].

From the last few years, research is going on the optimization of GaN-based LED structure design [14]–[17]. This optimization is beneficial to improve the efficiency in the symmetry of carrier transport, better injected charge carriers, confinement of carriers in the quantum wells which further enhances the radiative recombination rate leading to the breakthrough in the internal quantum efficiency (IQE) [18]–[20].

Due to the electron overflow, IQE and efficiency droop at high injection current face a critical issue [22]. Although the electron blocking layer (EBL) introduced between the p-region and active region can suppress the electron overflow[23], but the hole injection efficiency is also strongly affected because of positive polarization sheet charges formed at the heterointerface of the last quantum barrier (QB) and EBL[24]. Additionally due to high magnesium (Mg) activation energy in high Al content EBL, efficient p-doping is quite difficult [25]. Thus to mitigate these problems, in our paper we have used an EBL free multi-quantum well (MQW) UV-LED operating at ~354.6 nm wavelength which eliminates the formation of positive polarization sheet charges and shows a significantly enhanced hole injection and reduced electron leakage. We have presented a distinctive design of QB in GaN/AlGa<sub>N</sub> MQW by graded composition inside the entire barrier across [0001] axis. As a result, the performance of the proposed structure is remarkably improved, compared to the conventional UV-LED structure using an EBL and with square quantum barriers.

The design of LED structure and its numeral simulation framework is presented in Section 2 followed by Results and Analysis in Section 3. Finally, the Conclusion is drawn in Section 4.

## 2. DEVICE STRUCTURE AND NUMERICAL SIMULATION FRAMEWORK

In this study, the above-mentioned LED structures are numerically studied using the use of computer-aided simulation tool Silvaco ATLAS TCAD which is designed to analyze and optimize LEDs based on wurtzite semiconductor compounds[26].

A GaN/AlGa<sub>N</sub> LED with a peak wavelength of ~354.6 nm is presented in Fig. 1. The basic device structure considered as the conventional LED (LEDI) is constructed above a sapphire based substrate with a thickness of 80 μm followed by an undoped GaN buffer layer of thickness 1.2 μm, n-doped AlGa<sub>N</sub> coating layer (doping concentration:  $1 \times 10^{20}$  cm<sup>-3</sup>, width: 1.8 μm, Al content: 18%), four pairs of GaN (3 nm)/AlGa<sub>N</sub> (7 nm) MQW, p-doped AlGa<sub>N</sub> layer as EBL[27] (doping concentration:  $2 \times 10^{18}$  cm<sup>-3</sup>, width: 20 nm, Al content: 20%), p-doped AlGa<sub>N</sub> coating layer (doping concentration:  $1 \times 10^{18}$  cm<sup>-3</sup>, width: 180 nm, Al content: 15%) and finally p-doped GaN contact layer (doping concentration:  $2.5 \times 10^{18}$  cm<sup>-3</sup>, width: 80 nm). The quantum square barriers have 20% uniform Al composition.

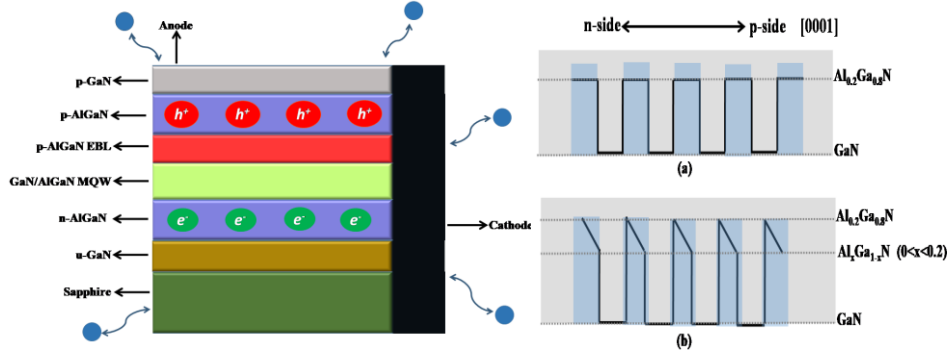


**Fig. 1** (a) Schematic diagrams of LEDI conventional GaN/AlGaN MQW with square QBs, (b) LEDII with triangular barriers

For the betterment of performance, the square barriers of LEDI have been optimized with graded composition. Along the n-side in each QB, the Al composition is integrated to 20% ( $Al_{0.26}Ga_{0.74}N$ ) while in the p-side the Al composition is defined by the variable  $x$  which is in the range ( $0 \leq x \leq 20\%$ ). The Al composition in each QB gradually reduces from 20% to  $x$  ( $Al_xGa_{1-x}N$ ,  $0 \leq x \leq 0.2$ ) across [0001] axis from n to p-side. The calculations are accomplished using the carrier mobilities of 90 (electrons) and 15 (holes)  $cm^2V^{-1}s^{-1}$  and the operating temperature is set as 300 K. The device with graded triangular barrier ( $x=0.02$  for reference) is considered as LEDII. The final EBL free UV-LED proposed structure with graded triangular barrier is considered as LEDIII which is the optimum goal of this paper. The Al composition in each QB is increased to 25% in the n-side while in the p-side the value of  $x$  is in the range ( $0 \leq x \leq 25\%$ ). The energy band gaps of the GaN and AlGaN used in the simulations are taken as 3.42 eV and 6.28 eV respectively. The respective radiative recombination rate of coefficient (COPT) are  $2 \times 10^{-10}$  and  $1.1 \times 10^{-10}$   $cm^3/s$ . The lattice constant of GaN is 0.3189 nm. The Auger coefficient and carrier lifetime have their default values as  $1 \times 10^{-34}$   $cm^6/s$  and  $1 \times 10^{-9}$  s respectively.

### 3. RESULTS AND ANALYSIS

#### 3.1. Internal Quantum Efficiency

The IQEs of the device with varying values of  $x$  in  $Al_xGa_{1-x}N$  in the graded QBs with respect to injection current are displayed in Fig. 2. As shown, efficiency of LEDI has the lowest value compared to the other cases with graded QB ( $0 \leq x \leq 0.2$ ). With decreasing band gap of  $Al_xGa_{1-x}N$  from n to p-side, the IQE at the same injection current remarkably raises.

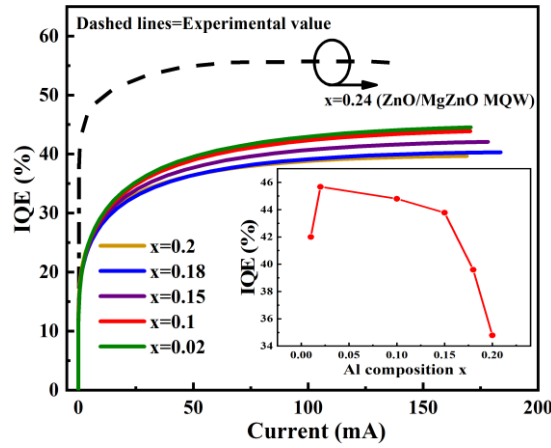
Due to better prospective, the efficiencies at 60 mA with respect to function  $x$  are displayed in the inset of Fig. 2. While reducing the values of  $x$  from 0.2 to  $\sim 0.02$ , the efficiency increases from 34.79% to 45.68% then vaguely minimizes while  $x$  approaches 0. This is because when Al-composition is further decreased to 0.02, band gap of  $Al_xGa_{1-x}N$  decreases which in turn increases the effective barrier heights for holes and electrons further. LEDII acquires 31.3% rise of efficiency at 60 mA compared to LEDI.

Fig. 3 show that the optimized EBL free device (LEDIII) has the highest IQE of 48.4% at 60 mA. LEDIII has 39.12% and 5.95% higher IQE than LEDI and LEDII respectively. The

efficiency droop is minimized from 13.87% (LEDI) to 10.22% (LEDII) and further to 7.72% (LEDIII) at the same current of 60 mA according to the equation given below:

$$Droop_{60\text{ mA}} = \frac{\eta_{peak} - \eta_{60\text{ mA}}}{\eta_{peak}} \quad (1)$$

This result establishes that the EBL free device with triangular barriers does contribute to the enhancement of IQE and decrease of efficiency droop. In order to validate our device model and parameters, the IQE is compared with the nearly available experimental result [28] as shown in Fig. 2.



**Fig. 2** Internal quantum efficiency vs. injected current with varying values of  $x$ . Inset: Values of IQEs as a function of  $x$ .

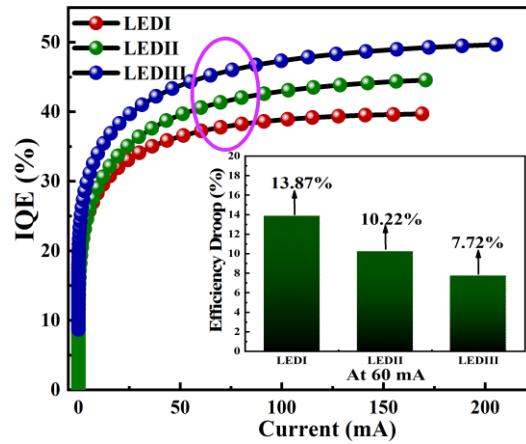


**Fig. 3** Internal quantum efficiency vs. injected current for all LEDs Inset: The efficiency droop for each LED at 60 mA current

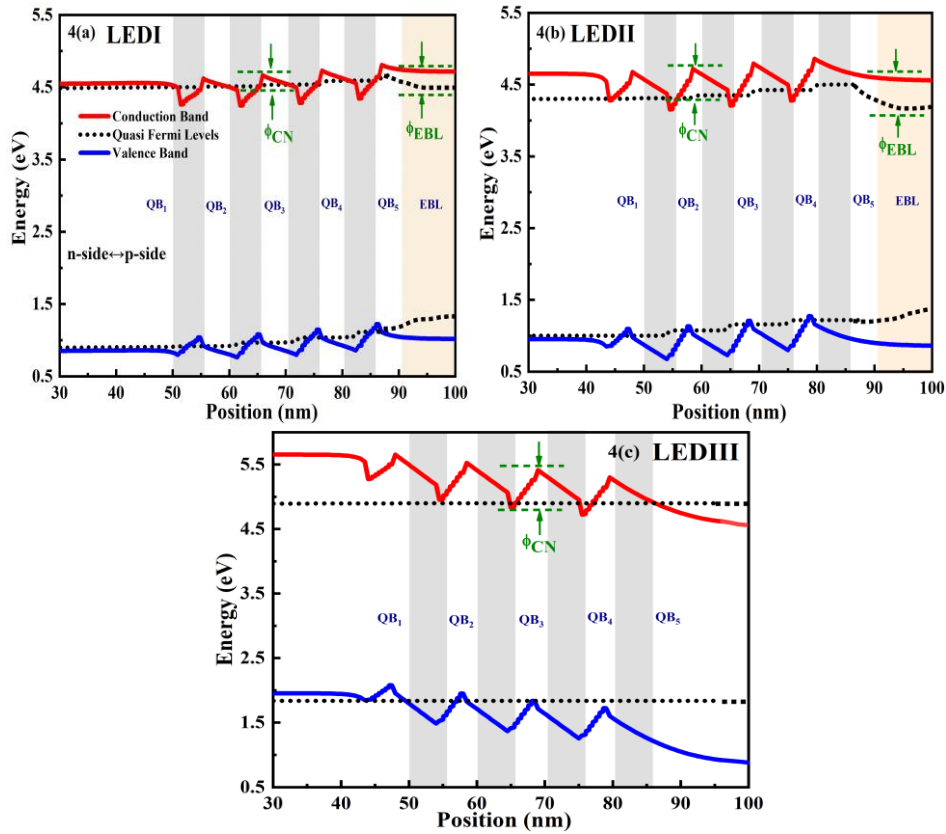
### 3.2. Energy Band Diagrams

Fig. 4 shows the calculated energy band diagrams for LEDI, LEDII and LEDIII at 60 mA injected current. The simulated results shown in Fig. 4(a)-(b) depict the dissimilarities and the tendency of variation of the energy band diagrams where the band gap of every QB is altered from uniform to graded composition. Band diagram of LEDI depicts a triangular designed shape because of the presence of internal polarization field and forward bias [29].

The energy band gap ( $E_g$ ) of  $Al_xGa_{1-x}N$  can be calculated as –

$$E_g(Al_xGa_{1-x}N) = E_g(AlN)x + E_g(GaN)(1 - x) - (1.3x(1 - x)) \quad (2)$$

where  $\rightarrow E_g(AlN) =$  Band gap energy of  $AlN = 6.2$  eV,  $E_g(GaN) =$  Band gap energy of  $GaN = 3.42$  eV [30]



**Fig. 4** Energy Band diagram of active region of GaN/AlGaN MQW for (a) LEDI, (b) LEDII and (c) LEDIII

This mathematical formula shows that the band gap of  $Al_xGa_{1-x}N$  decreases with a decrease in the Al composition. Hence the band gap of every QB reduces while moving from n to p-side, thus influencing the effective barrier heights for electrons as well as holes. The formation of the hole depletion region due to the positive polarization sheet charges

interface at LQB/EBL lessens the hole injection efficiency in LEDII [24]. This problem can be overcome by removing the EBL from LEDII.  $\phi_{CN}$  and  $\phi_{EBL}$  are the effective conduction band barrier height (CBBH) at corresponding barrier (n) and EBL respectively. Displayed in Fig. 4(b), the values of  $\phi_{CN}$  for all QBs i.e.  $\phi_{c1}-\phi_{c5}$  are 370.8 meV, 408.2 meV, 442.2 meV, 367 meV and  $\phi_{EBL}$  is 468.9 meV for LEDII which is much higher than  $\phi_{EBL}$  for LEDI (257.1 meV). The  $\phi_{CN}$  values in the proposed EBL-free LEDIII i.e.  $\phi_{c1}-\phi_{c5}$  are 460.2 meV, 618.3 meV, 505.2 meV and 632.1 meV, respectively. The higher and progressively increased  $\phi_{CN}$  in LEDIII constructively confine the electrons in the active region and effectively resist the electron overflow into p-region. This leads to the significantly reduced non-radiative recombination in p-region and enhances hole injection into the active region.

### 3.3. Carrier Concentration

The electron as well as hole concentration distribution in the MQW of various LEDs is displayed in Fig. 5 to further understand the reason behind the tremendous performance improvement in LEDIII. LEDI indicates a hole concentration of  $10.4 \times 10^{18} \text{ cm}^{-3}$  in the initial quantum well from n to p-side which is much lower than LEDII ( $16.9 \times 10^{18} \text{ cm}^{-3}$ ). These results specify that graded QB LED has superior hole transport lessening the hole concentration. The distribution of electrons, as observed in graded QB LED, appears to have better uniformity, compared to LEDI, which may proportionate to superior transportation of

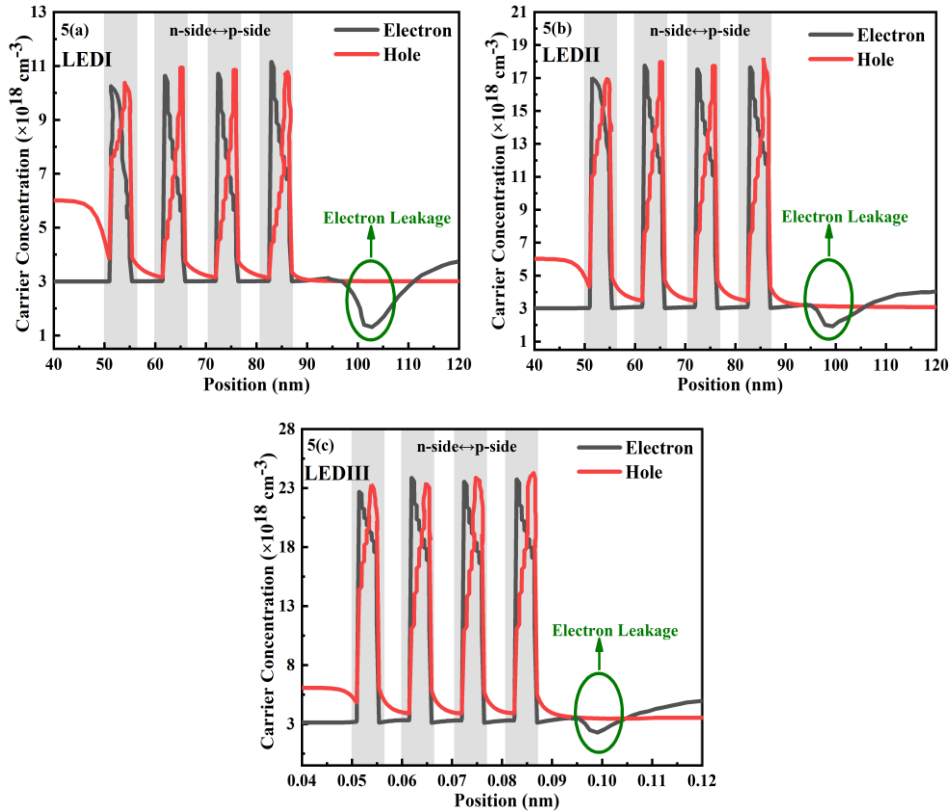


Fig. 5 Carrier concentration of (a) LEDI, (b) LEDII and (c) LEDIII

holes [31]. The electron leakage in LEDIII is notably mitigated and lower than LEDII which blocks the undesired recombination of electrons with incoming holes in the p-region. Subsequently, LEDIII has higher electron ( $22.6 \times 10^{18} \text{ cm}^{-3}$ ) and hole ( $23.2 \times 10^{18} \text{ cm}^{-3}$ ) concentration throughout the active region, compared to LEDII.

### 3.4. Radiative Recombination

The distribution of radiative recombination in the active region at an injection current of 60 mA is simulated and illustrated in Fig. 6. The radiative recombination distribution in LEDII is more uniform compared to LEDI. In LEDI, radiative recombination in the primary QW has a recombination rate of  $2.38 \times 10^{28} \text{ cm}^{-3}\text{s}^{-1}$ . This is probably due to the deficient spatial distribution overlap between holes and electrons [32]. The electrostatic field in MQWs of LEDIII is lower than LEDII that supports the spatial overlap of electron-hole wave functions which improves the radiative recombination process [33]. Thus, the recombination rate of LEDIII is increased by  $\sim 136.7\%$  compared to LEDII. As shown in Fig. 5, most electrons still accumulate in the initial well, while the hole concentration in the last well is less than that in the previous wells. However, in conventional LED, both holes and electrons are centred at the wells close to p-GaN, hence the radiative recombination is extremely effective at that location. Above outcomes suggest that in order to diminish the droop behaviour of LED without deteriorating total recombination, more attention has to be given to the spatial distribution between the holes and electrons [34].

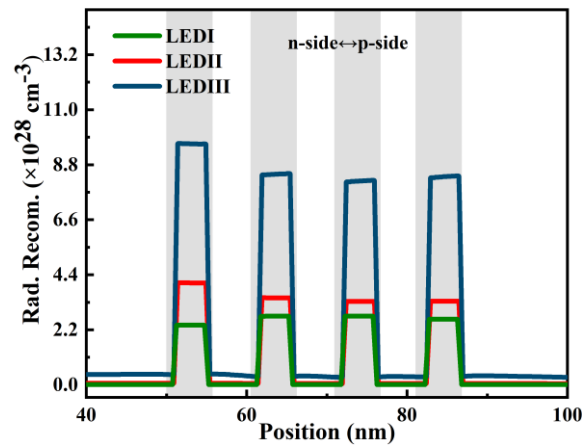
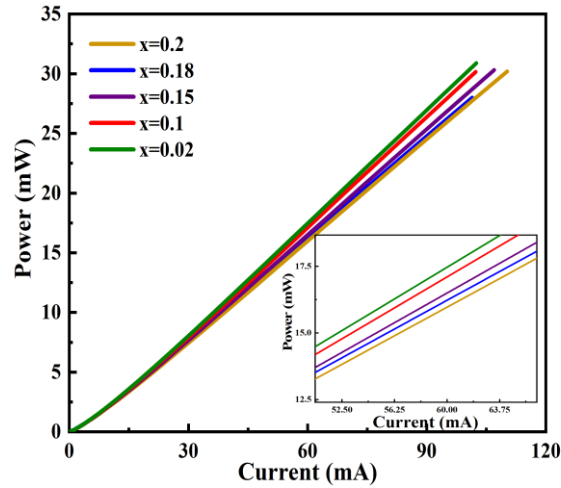


Fig. 6 Radiative Recombination Rate of all LED samples

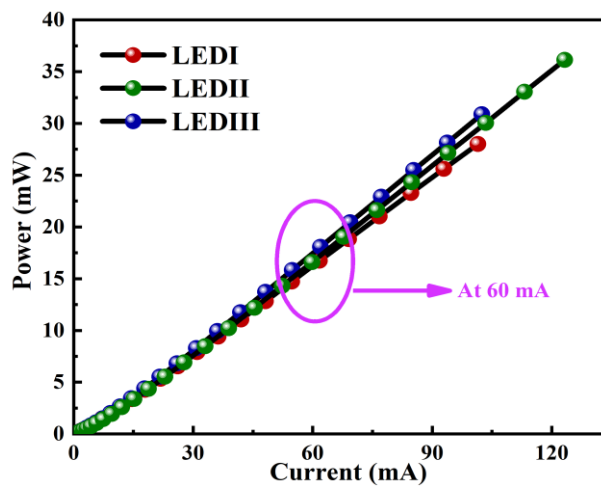
### 3.5. Power

Fig. 7 illustrates the luminous power vs. current for LEDI and LEDII. The light output is observed to be amplified with decrease in the value of  $x$  because graded QB benefits from superior electron confinement and larger hole injection efficiency. These superior optical properties are also attributed to the decrease in the polarization field in the MQW [35]. This improved power means that more carriers will recombine in the QW of graded QB LED thus effectively improving the light efficiency of GaN/AlGaN LED [36]. Furthermore, as shown in Fig. 8, the output power of LEDIII is remarkably increased to

18.075 mW from 16.723 mW (LEDI) at 60 mA current injection i.e.  $\sim 8.084\%$  enhancement. The normalised power spectral density of the three devices is displayed in Fig. 9. Conventional LEDI has stronger Quantum-confined stark effect (QCSE) induced by the spontaneous and piezoelectric fields in the MQW layers which shows an obvious screening effect and band-filling effect. This results in a blue-shift in LEDI. From Fig. 9, LEDIII shows a red shift of  $\sim 5$  nm because of negligent presence of QCSE.



**Fig. 7** Behaviour of luminous power versus forward current with varying values of  $x$ . Inset: Clearer view of power at 60 mA current



**Fig. 8** Luminous Power as a function of injected current for all LEDs

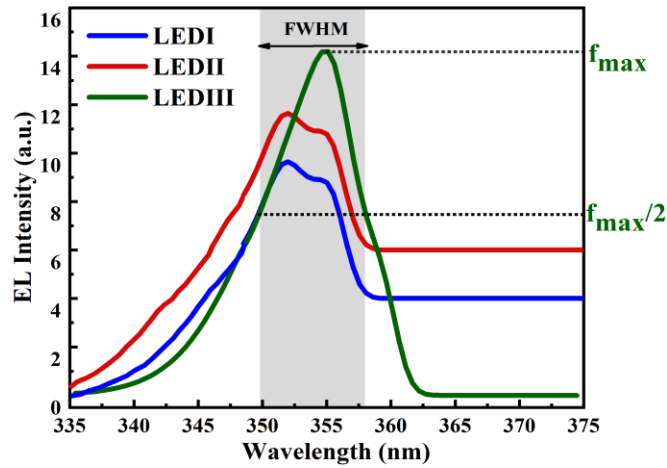


**Fig. 9** Room temperature EL spectra of all the LED devices vs. wavelength

#### 4. CONCLUSION

To summarize, EBL free UV-LED of GaN/AlGaN MQWs with specially designed graded QBs are numerically simulated. After reducing the band gap of AlGa<sub>N</sub> across [0001] axis from n towards p region in every QB, the efficiencies of the device enhance. The upgraded LED having  $x=0.02$  (LEDII) acquires topmost IQE of ~45.68 % at 60 mA which is 31.3% more compared to the conventional one (LEDI) with square barriers. The reason behind this improvement is attributed to the modified energy band diagrams in the graded QBs. Moreover, we have numerically demonstrated EBL free UV-LED graded QB structure and observed that it can effectively suppress electron overflow, support enhanced hole injection into the LED active region as compared to the conventional LED. The hole transport in MQWs was notably intensified at current of 60 mA which is beneficial for droop reduction. The efficiency droop was decreased from 13.87% in conventional LED to only 10.22% in graded QB LED and further to 7.72% in the proposed EBL free LED. The proposed LED has an 8.084% increase in the luminous power at an injection current of 60 mA as compared to conventional LED and 39.12% rise in the efficiency. We believe that the EL performance of the LEDs based on GaN materials can be further improved through elaborate device design and carefully considering the varying carrier transport characteristics of GaN based LEDs, which show different conduction-to-valence band-offset ratios in their MQW structures.

**Acknowledgement:** *This work is one of the outcomes of DST-SERB, Govt. of India sponsored MATRICS Project No MTR/2021/000370 which is duly acknowledged for support.*

## REFERENCES

- [1] S. Das, T. R. Lenka, F. A. Talukdar and R. T. Velpula, "Carrier Transport and Radiative Recombination Rate Enhancement in GaN/AlGa<sub>N</sub> Multiple Quantum Well UV-LED Using Band Engineering for Light Technology", In Proceedings of the 2nd International Conference on Micro and Nanoelectronics Devices, Circuits and Systems, MNDCS 2022, pp. 1–11.
- [2] M. Usman, U. Mushtaq, M. Munsif, A. R. Anwar and M. Kamran, "Enhancement of the optoelectronic performance of p-down multiquantum well N-GaN light-emitting diodes", *Phys. Scr.*, vol. 94, no. 10, p. 105808, 2019.
- [3] H. Tao, S. Xu, J. Zhang, P. Li, Z. Lin and Y. Hao, "Numerical Investigation on the Enhanced Performance of N-Polar AlGa<sub>N</sub>-Based Ultraviolet Light-Emitting Diodes with Superlattice p-Type Doping", *IEEE Trans. Electron Devices*, vol. 66, no. 1, pp. 478-484, 2019.
- [4] S. Das *et al.*, "Effects of polarized-induced doping and graded composition in an advanced multiple quantum well InGa<sub>N</sub>/Ga<sub>N</sub> UV-LED for enhanced light technology", *Eng. Res. Express*, vol. 4, no. 1, p. 015030, 2022.
- [5] Y. Nagasawa and A. Hirano, "A review of AlGa<sub>N</sub>-based deep-ultraviolet light-emitting diodes on sapphire", *Appl. Sci.*, vol. 8, no. 8, p. 1264, 2018.
- [6] M. Usman *et al.*, "Zigzag-shaped quantum well engineering of green light-emitting diode", *Superlattices Microstruct.*, vol. 132, p. 106164, 2019.
- [7] G. Kim, J. H. Kim, E. H. Park, D. Kang and B.-G. Park, "Extraction of recombination coefficients and internal quantum efficiency of GaN-based light emitting diodes considering effective volume of active region", *Opt. Express*, vol. 22, no. 2, p. 1235, 2014.
- [8] H. Hu, S. Zhou, X. Liu, Y. Gao, C. Gui and S. Liu, "Effects of GaN/AlGa<sub>N</sub>/Sputtered AlN nucleation layers on performance of GaN-based ultraviolet light-emitting diodes", *Sci. Rep.*, vol. 7, p. 44627, 2017.
- [9] S. Zhou, X. Liu, H. Yan, Z. Chen, Y. Liu and S. Liu, "Highly efficient GaN-based high-power flip-chip light-emitting diodes", *Opt. Express*, vol. 27, no. 12, pp. A669–A692, 2019.
- [10] X. Zhao, B. Tang, L. Gong, J. Bai, J. Ping and S. Zhou, "Rational construction of staggered InGa<sub>N</sub> quantum wells for efficient yellow light-emitting diodes", *Appl. Phys. Lett.*, vol. 118, no. 18, p. 182102, 2021.
- [11] S. Zhou *et al.*, "Numerical and experimental investigation of GaN-based flip-chip light-emitting diodes with highly reflective Ag/TiW and ITO/DBR Ohmic contacts", *Opt. Express*, vol. 25, no. 22, p. 26615, 2017.
- [12] Y. Meng *et al.*, "Growth and characterization of amber light-emitting diodes with dual-wavelength InGa<sub>N</sub>/Ga<sub>N</sub> multiple-quantum-well structures", *Mater. Res. Express*, vol. 6, no. 8, p. 0850c8, 2019.
- [13] C. H. Wang *et al.*, "Efficiency droop alleviation in InGa<sub>N</sub>/Ga<sub>N</sub> light-emitting diodes by graded-thickness multiple quantum wells", *Appl. Phys. Lett.*, vol. 97, no. 18, p. 181101, 2010.
- [14] Z. Lin, X. Chen, Y. Zhu, X. Chen, L. Huang and G. Li, "Influence of Thickness of p-InGa<sub>N</sub> Layer on the Device Physics and Material Qualities of GaN-Based LEDs With p-GaN/InGa<sub>N</sub> Heterojunction", *IEEE Trans. Electron Devices*, vol. 65, no. 12, pp. 5373–5380, 2018.
- [15] M. Usman, A. R. Anwar, M. Munsif, S. Malik and N. U. Islam, "Analytical analysis of internal quantum efficiency with polarization fields in GaN-based light-emitting diodes", *Superlattices Microstruct.*, vol. 135, p. 106271, 2019.
- [16] H. Hu *et al.*, "Boosted ultraviolet electroluminescence of InGa<sub>N</sub>/AlGa<sub>N</sub> quantum structures grown on high-index contrast patterned sapphire with silica array", *Nano Energy*, vol. 69, p. 104427, 2020.
- [17] X. Fan, S. Xu, H. Tao, R. Peng, J. Du, Y. Zhao, J. Zhang, J. Zhang and Y. Hao, "Improved Performance of GaN-Based Ultraviolet LEDs with the Stair-like Si-Doping n-GaN Structure", *MDPI*, vol. 11, no. 10, p. 1203, 2021.
- [18] M. H. Kim *et al.*, "Origin of efficiency droop in GaN-based light-emitting diodes", *Appl. Phys. Lett.*, vol. 91, no. 18, pp. 1-4, 2007.
- [19] J. H. Park *et al.*, "Enhanced overall efficiency of GaInN-based light-emitting diodes with reduced efficiency droop by Al-composition-graded AlGa<sub>N</sub>/Ga<sub>N</sub> superlattice electron blocking layer", *Appl. Phys. Lett.*, vol. 103, no. 6, 2013.
- [20] C. Sheng Xia, Z. M. Simon Li, W. Lu, Z. Hua Zhang, Y. Sheng and L. Wen Cheng, "Droop improvement in blue InGa<sub>N</sub>/Ga<sub>N</sub> multiple quantum well light-emitting diodes with indium graded last barrier", *Appl. Phys. Lett.*, vol. 99, no. 23, p. 233501, 2011.
- [21] S. Das, T. R. Lenka, F. A. Talukdar, R. T. Velpula, H. P. T. Nguyen and C. Engineering, "Carrier Transport and Radiative Recombination Rate Enhancement in GaN / AlGa<sub>N</sub> Multiple Quantum Well UV-LED using Band Engineering for Light Technology", In: Lenka, T.R., Misra, D., Fu, L. (eds) Micro and Nanoelectronics Devices, Circuits and Systems. Lecture Notes in Electrical Engineering, vol. 904. Springer, Singapore. pp. 187-198.

- [22] J. Cho, E. F. Schubert and J. K. Kim, "Efficiency droop in light-emitting diodes: Challenges and counter measures", *Laser Photonics Rev.*, vol. 7, no. 3, pp. 408-421, 2013.
- [23] H. Hirayama *et al.*, "222-282 nm AlGa<sub>N</sub> and InAlGa<sub>N</sub>-based deep-UV LEDs fabricated on high-quality AlN on sapphire", *Phys. Status Solidi Appl. Mater. Sci.*, vol. 206, no. 6, pp. 1176-1182, 2009.
- [24] C. Chu *et al.*, "On the origin of enhanced hole injection for AlGa<sub>N</sub>-based deep ultraviolet light-emitting diodes with AlN insertion layer in p-electron blocking layer", *Opt. Express*, vol. 27, no. 12, p. A620, 2019.
- [25] M. L. Nakarmi, N. Nepal, J. Y. Lin and H. X. Jiang, "Photoluminescence studies of impurity transitions in Mg-doped AlGa<sub>N</sub> alloys", *Appl. Phys. Lett.*, vol. 94, no. 9, pp. 1-5, 2009.
- [26] S. Clara, "Silvaco User's Manual DEVICE SIMULATION SOFTWARE," no. October, 2004, [Online]. Available: [www.silvaco.com](http://www.silvaco.com).
- [27] B.-C. Lin *et al.*, "Hole injection and electron overflow improvement in InGa<sub>N</sub>/Ga<sub>N</sub> light-emitting diodes by a tapered AlGa<sub>N</sub> electron blocking layer", *Opt. Express*, vol. 22, no. 1, p. 463, 2014.
- [28] J. Li *et al.*, "Carrier transport improvement in ZnO/MgZnO multiple-quantum-well ultraviolet light-emitting diodes by energy band modification on MgZnO barriers", *Opt. Commun.*, vol. 459, 2020.
- [29] K. Mehta *et al.*, "Theory and design of electron blocking layers for III-N-based laser diodes by numerical simulation", *IEEE J. Quantum Electron.*, vol. 54, no. 6, pp. 1-11, 2018.
- [30] H. Hirayama, S. Fujikawa and N. Kamata, "Recent progress in AlGa<sub>N</sub>-based deep-UV LEDs", *Electron. Commun. Japan*, vol. 98, no. 5, pp. 1-8, 2015.
- [31] R. Charash *et al.*, "Carrier distribution in InGa<sub>N</sub>/Ga<sub>N</sub> tricolor multiple quantum well light emitting diodes", *Appl. Phys. Lett.*, vol. 95, no. 15, pp. 2007-2010, 2009.
- [32] S. Zhou, J. Lv, Y. Wu, Y. Zhang, C. Zheng and S. Liu, "Reverse leakage current characteristics of InGa<sub>N</sub>/Ga<sub>N</sub> multiple quantum well ultraviolet/blue/green light-emitting diodes", *Jpn. J. Appl. Phys.*, vol. 57, no. 5, p. 051003, 2018.
- [33] Y. A. Yin, N. Wang, G. Fan and Y. Zhang, "Investigation of AlGa<sub>N</sub>-based deep-ultraviolet light-emitting diodes with composition-varying AlGa<sub>N</sub> multilayer barriers", *Superlattices Microstruct.*, vol. 76, pp. 149-155, 2014.
- [34] J. Chang *et al.*, "AlGa<sub>N</sub>-based multiple quantum well deep ultraviolet light-emitting diodes with polarization doping", *IEEE Photonics J.*, vol. 8, no. 1, pp. 1-7, 2016.
- [35] T. Y. Wang *et al.*, "AlGa<sub>N</sub>-based deep ultraviolet light emitting diodes with magnesium delta-doped AlGa<sub>N</sub> last barrier", *Appl. Phys. Lett.*, vol. 117, no. 25, p. 251101, 2020.
- [36] H. Li, C. J. Chang, S. Y. Kuo, H. C. Wu, H. Huang and T. C. Lu, "Improved performance of near UV Ga<sub>N</sub>-Based light emitting diodes with asymmetric triangular multiple quantum wells", *IEEE J. Quantum Electron.*, vol. 55, no. 1, pp. 1-4, 2019.